



1 **Changes in extreme precipitation patterns over the greater**
2 **Caribbean and teleconnection with large-scale sea surface**
3 **temperature**
4

5 Carlo Destouches^{1,2}, Arona Diedhiou², Sandrine Anquetin², Benoit Hingray², Armand Pierre¹, Dominique Boisson¹
6 Adermus Joseph¹

7 ¹Université d'Etat d'Haïti, Faculté des Sciences, LMI CARIBACT, URGéo, Port-au-Prince, Haïti

8 ² Univ. Grenoble Alpes, IRD, CNRS, Grenoble INP, IGE, F-38000 Grenoble, France

9
10 *Correspondence to:* Carlo Destouches(carlo.destouches@univ-grenoble-alpes.fr)

11
12
13 **Abstract:**

14 This study examines changes in extreme precipitation over the greater Caribbean and their correlation with large-scale
15 sea surface temperature (SST) for the period 1985 to 2015. The data used for this study were derived from two satellite
16 products: Climate Hazards Group InfraRed Precipitation (CHIRPS) and NOAA DOISST (Daily Optimum
17 Interpolation Sea Surface Temperature version 2.1) with resolutions of 5 km and 25 km, respectively. Then, change
18 in the characteristics of six(6) extreme precipitation indices defined by the WMO ETCCDI (World Meteorological
19 Organization Expert Team on Climate Change Detection and Indices) is analyzed, and Spearman's correlation
20 coefficient has been used and evaluated by t-test to investigate the influence of a few large-scale SST indices: (i)
21 Caribbean Sea Surface Temperature (SST-CAR); (ii) Tropical South Atlantic (TSA); (iii) Southern Oscillation Index
22 (SOI); (iv) Northern Oscillation Index (NAO). The results show that at the regional scale, +NAO contributes
23 significantly to a decrease in heavy precipitation (R95p), daily precipitation intensity (SDII), and total precipitation
24 (PRCPTOT), whereas +TSA is associated with a significant increase in daily precipitation intensity (SDII). At an
25 island scale, in Puerto Rico and southern Cuba, the positive phase of +TSA, +SOI, and +SST-CAR is associated with
26 an increase in daily precipitation intensity (SDII) and heavy precipitation (R95p). However, in Jamaica and northern
27 Haiti, the positive phases of +SST-CAR and +TSA are also associated with increased indices (SDII, R95p). In
28 addition, the SST warming of the Caribbean Sea surface temperature and the positive phase of the Southern Oscillation
29 (+SOI) significantly increases with the number of rainy days (RR1) and the maximum duration of consecutive rainy
30 days (CWD) over the Dominican Republic and in southern Haiti.

31
32 **Keywords:** Caribbean region; Greater Caribbean; Extreme precipitation; Climate variability; Sea surface temperature
33
34
35
36
37
38



39 1 Introduction

40 Over the past three decades, the climatic hazards to which the Caribbean Basin has been exposed include recurrent
41 cyclonic and hydrometeorological hazards, characterized by increasing intensities (Joseph, 2006). The economic cost
42 of 250 storms and floods over a 40-year period (1970 to 2009) for 12 Caribbean countries amounted to US\$19.7 billion
43 in 2010, representing an annual average of 1% of gross domestic product (GDP) (Burgess et al., 2018). The most
44 dreadful damage caused by these hydroclimatic events includes George in 1998, with 1,000 victims in the Dominican
45 Republic and losses estimated at 14% of GDP, equivalent to approximately half the exports made that year (Naciones
46 Unidas, Comision economica para America Latima y el Caribe, 1988); Matthew in Haiti (October 2016), with over
47 500 dead, 128 missing, 439 injured and 2.1 million people affected, including 895,000 children (De Giogi et al., 2021)
48 . Also, Hurricane Dorian caused property damage estimated at 2.5 billion USD when it came to rest over the Bahamas
49 as a Category 5 storm in September 2019, rendering nearly 3,000 homes uninhabitable and causing extensive damage
50 to hospitals, schools, and fisheries (Panamerican Health Organisation, 2019). A severe drought episode affected the
51 island of Caribbean from October 2019 to mid-2020, causing water shortages, bushfires, and agricultural losses. In
52 Saint Vincent and the Grenadines, the 2020 drought was considered the worst of the 50 years (Nurse, 2020). The Inter-
53 American Development Bank predicts that the Caribbean could face climate-related losses of over \$22 billion per year
54 by 2050 (Inter-American Development Bank, 2014).

55 In response to the climate extremes that are further weakening the island states of the Caribbean region, already in a
56 situation of extreme socio-economic precariousness, several studies have been carried out in parallel to understand
57 the associated physical processes and anticipate the evolution of these extreme climatic events. Research into the
58 Caribbean climate goes back to the second half of the twentieth century and has focused mainly on rainfall patterns
59 (Curtis et al., 2008), as well as on the overall description of rainy seasons (Griffiths et al., 1982).

60 A more detailed study of the climate of the Caribbean was performed in 2001 and 2002 using indices derived from
61 daily data to detect climate change (Peterson et al., 2001; Frich et al., 2002). This approach, which uses indices defined
62 by the World Meteorological Organization's group of experts to characterize precipitation and temperature extremes,
63 has enabled several studies to examine the state of climate extremes over the Caribbean (Stephenson et al., 2014;
64 McLean et al., 2015). The results of these previous assessments agree that the frequency and intensity of climate
65 extremes over the Caribbean have increased over the last 30 years (Stephenson et al., 2014; Peterson et al., 2002a;
66 Beharry et al., 2015; Dookie et al., 2019), and will continue to do so until the end of the century (Taylor et al., 2018;
67 Vichot-Llano et al., 2021; Hall et al., 2013; Almazroui et al., 2021; McLean et al., 2015).

68 Climate teleconnections, the remote forcing of a region far from the source of disturbance, whether simultaneous or
69 time-lagged (Mariami et al., 2018; Rodrigues et al., 2021), are generally derived from variations in sea surface
70 temperature (SST) or atmospheric pressure at seasonal to interdecadal scales. Several of these have been shown to
71 play a major role in modifying global weather patterns (Hurrell et al., 1995; Martens et al., 2018).



72 Previous studies have also shown the effect of east-west gradients in SST anomalies in the tropical Pacific and Atlantic
73 on precipitation in the Caribbean, with a tendency for a warm Atlantic and a cold Pacific to favor precipitation in the
74 Caribbean (Taylor et al., 2002a; Gimeno et al., 2011). Studies in (Enfiel et al., 2001; IPCC, 2007) also found that the
75 monthly AMO index is an SST signal in the North Atlantic that influences the decadal-scale variability in precipitation.
76 In addition, (Peterson et al., 2022) analyzed the link between SST, air temperature, and precipitation extremes over
77 the Caribbean using ground-based observations. They showed that the extreme precipitation index (SDII) averaged
78 over the Caribbean has a strong correlation with SST over the Caribbean and the entire tropical North Atlantic Ocean.
79 The work of (Stephenson et al., 2014) examined the influence of Atlantic Multidecadal Oscillation (AMO) on extreme
80 precipitation from a ground-based observation network in the Caribbean. These results show that the AMO influences
81 the variability of extreme temperature and precipitation events; however, further research is needed. In addition, the
82 effects of teleconnections caused by large-scale SST on weather conditions are expected to become more extreme in
83 the future due to climate change (Mariami et al., 2018).

84 In this context, the aim of this study was to examine the remote impact of the tropical Pacific Ocean, Atlantic Ocean,
85 and Caribbean Sea on observed changes in the tropical islands of the Greater Antilles, particularly the links between
86 extreme precipitation indices and large-scale sea surface indices. This paper is organized into five sections: Section 1
87 presents the study area and the associated climatology. Sections 2 and 3 describe the spatio-temporal variability of
88 extreme precipitation indices at regional and local scales and the influence of SST indices on extreme precipitation.
89 The last sections (4-5) present the discussion and conclusion.

90

91 **2 Study area and Data**

92 **2.1 Study area**

93 The Greater Antilles is a region between North and South America made up of four islands bordered by the Caribbean
94 Sea to the south and the Atlantic Ocean to the east (Fig.1). These islands include Cuba, Hispaniola, Jamaica, and
95 Puerto Rico. They have a monthly rainfall cycle characterized by two peaks: the first in May and the second between
96 September and November. The climatology of monthly rainfall in the Greater Antilles is strongly influenced by the
97 subtropical North Atlantic anticyclone (Davis et al., 1997), the easterly winds of the intertropical zone, and the trade
98 winds (Cook et al., 2010). They were also influenced by the intertropical convergence zone (ITCZ) (Hastenrath et al.,
99 2002), with maximum precipitation in May (fig.1b). Heavy autumn rainfall in the Greater Antilles (supl.fig.2d) is
100 generally associated with North Atlantic tropical cyclones, 85% of which are of high intensity and originate from
101 African easterlies (Agudelo et al., 2011; Thorncroft et al., 2001) under warm Atlantic basin conditions. The total
102 annual precipitation in the Greater Antilles depends on land-sea interactions (breezes) and topography (fig.1a). The
103 spatial distribution of the total annual precipitation in the Greater Antilles, particularly on the islands, is not
104 homogeneous because of topography (Moron et al., 2015). Precipitation is relatively high (2,000-24,000< mm/year)



105 at higher altitudes and in wind-exposed areas (fig.1b). In contrast, annual precipitation can reach 500 mm/year in
106 leeward areas (Daly et al., 2003).

107

108

109 **2.2 Satellite data**

110 This study was conducted using two satellite datasets: NOAA DOISST Sea surface temperature data and CHIRPSv2
111 data. The CHIRPSv2 data (Climate Hazards Group Infrared Precipitation with Stations data version 2) are quasi-
112 global daily precipitation data (50S-50N) with a resolution of 0.050, available over a period from 1981 to 2022(Funk
113 et al., 2015). Based on the techniques used by NOAA for estimating precipitation in the thermal infrared (Love et al.,
114 2004), the CHIRPS database was built from precipitation estimates based on cold cloud duration observations, and a
115 fusion incorporating monthly CHPClim (Funk et al., 2015a) (Climate Hazards Group Precipitation Climatology
116 (CHPClim) precipitation data, and in situ data from ground observation networks. TRMM 3B42v7 (Tropical Rainfall
117 Measuring Mission Multi-Satellite Precipitation Analysis) satellite products were also used to calibrate and reduce the
118 bias in the estimates. The results of global and regional validation studies showed that CHIRPS can be used to quantify
119 the hydrological impacts of decreasing rainfall and increasing air temperatures in the Greater Horn of Africa (Funk et
120 al., 2015). In addition, the performance of CHIRPS, evaluated over certain regions of the Americas, has demonstrated
121 its ability to reproduce the mean climate as well as its capacity to estimate extreme precipitation events. For example,
122 in Colombia, the best results were obtained on a daily and monthly scale over the Magdalena River Basin (the largest
123 in Colombia) (Baez-Villanueva et al., 2018). CHIRPS data are suitable for our study, as their performance over the
124 Caribbean, particularly the Greater Antilles, has shown their ability to estimate heavy precipitation (Bathelemy et al.,
125 2022).

126 NOAA DOISST (Daily Optimum Interpolation Sea Surface Temperature version 2.1) data are daily sea surface
127 temperature data derived from a combination of in situ sea surface temperature (SST) data obtained from ships and
128 buoys and sea surface temperatures obtained from the Advanced Very High Resolution Radiometer (AVHRR)(Huang
129 et al., 2021). This satellite product is the result of a global file of 0.250-degree grid points, available over the period
130 1981-2020.

131

132 **3. Methodology**

133 To provide countries with information on extreme weather events, a group of World Meteorological Organization
134 experts (ETCCDI: Expert Team on Climate Change Detection and Indices) defined 27 indices to characterize extreme
135 precipitation and temperature events in terms of their frequency, amplitude, and duration (Peterson et al., 2001).
136 Although the proposed method includes numerous indices based on percentiles, with thresholds set to assess extremes



137 that generally occur a few times a year and not necessarily high-impact events, it has paved the way for numerous
138 research projects in the Caribbean (Stephenson et al., 2014; McLean et al., 2015). Six (6) extreme precipitation indices
139 (Table 1) were calculated: total annual precipitation (PRCPTOT), number of rainy days (RR1), intensity of rain events
140 (SDII), and heavy precipitation (R95p), calculated in relation to a threshold corresponding to the 95th percentile of
141 the daily precipitation distribution, maximum number of consecutive wet days (CWD), and maximum number of
142 consecutive dry days (CDD).

143 The spatiotemporal evolution of extreme precipitation in the Greater Antilles was investigated by analyzing the
144 interannual variability of extreme precipitation index anomalies over a long period (1985-2015) and the change in
145 percentage variations in extreme precipitation indices at decadal timescales. To characterize the percentage variations,
146 we chose the (P_{ij}) index, which is already used in the study (An et al., 2023), whose equation is presented hereafter.

$$147 \quad P_{ij} = \left(\frac{P_{i(j+1)}}{P_{ij}} - 1 \right) \times 100 \quad (1)$$

148 where P_{ij} is the average extreme precipitation index for the j -th decade at the i -th location, and $P_{i(j+1)}$ is the average
149 extreme precipitation index for the $(j+1)$ -th decade at the i -th location.

150 Then, as the variability of precipitation in the region is known to be linked to SST in the tropical Pacific and
151 Atlantic (Gimeno et al., 2011; Enfiel et al., 2001), we selected four large-scale SST indices, namely the Southern
152 Oscillation Index (SOI), the North Atlantic Oscillation (NAO) (Jones et al., 1997), the Tropical South Atlantic
153 Anomaly Index (TSA), and the SST over the Caribbean Sea (SST-CAR), and investigated the teleconnection between
154 these indices and the precipitation extremes in the region. Detailed descriptions and estimates of these SST indices
155 are available in (<https://psl.noaa.gov/data/climateindices/list/#Nina34>).

156 The teleconnection between SST and extreme precipitation indices was assessed using Spearman's correlation
157 coefficient analysis. Such an analysis with Spearman correlation has already been carried out in the study of
158 (Khadgarai et al., 2021), as well as in other studies on spatial correlation (Chen et al., 2015; Sunilkumar et al., 2016)
159 . This coefficient was interpreted over a closed interval between -1 and 1. A value of zero (0) indicates that there is no
160 relationship between the two variables; a negative value (negative correlation) indicates that when one variable
161 increases, the other decreases, while a positive value (positive correlation) indicates that the two variables vary in the
162 same direction. Spearman's correlation coefficient is calculated using the following equation:

$$163 \quad r_{\text{spearman}} = \frac{\sum_{i=1}^n (R_i - \bar{R})(S_i - \bar{S})}{\sqrt{\sum_{i=1}^n (R_i - \bar{R})^2 \sum_{i=1}^n (S_i - \bar{S})^2}} \quad (2)$$

164 where r_{spearman} is the correlation coefficient, $R_i = \text{rang}(X_i)$, $S_i = \text{rang}(Y_i)$ are respectively the data ranks of Variables
165 X and Y (X: Extreme precipitation index, Y: Large-scale SST index).



166 To test the significance of the relationship, that is, whether the two variables are really correlated or not, we use the t-
167 test for a threshold of 0.05 or less. This involves testing the two hypotheses (H0 and H1) based on the value of t to
168 deduce the probability of observing a result that deviates as much as expected from the correlation. The formula for
169 calculating the value of t using Spearman's correlation is as follows:

$$170 \quad t_{n-2} = \frac{r_{spearman}}{\sqrt{1-r_{spearman}^2}} \sqrt{n-2} \quad (3)$$

171

172 **4 Results**

173 **4.1 Changes in precipitation extreme indices**

174 The observed changes in total annual precipitation (PRCPTOP), number of rainy days (RR1), rainfall intensity (SDII),
175 contribution of heavy rainfall (R95p), and maximum duration of consecutive rainy days (CWD) and dry days (CDD)
176 in the Greater Antilles over the three decades (1985-1994, 1995-2004, 2005-2015) are shown in fig. 2. The first decade
177 of 1985-1994 was generally marked by a decline in total annual precipitation (fig.2a), associated with a decrease in
178 the number of rainy days (fig. 2b), a decrease in the average rainfall intensity (fig. 2c), a decrease in the contribution
179 of heavy rainfall (fig. 2d), and in the length of wet and dry spells (fig. 2e, 2f). The second decade 1995-2004, was
180 mainly characterized by an increase in rainfall associated with an increase in rainfall intensity, the contribution of
181 heavy rainfall, and the length of dry spells. The last decade 2005-2015, was characterized by a wet period (until 2012)
182 followed by a dry period. Except for 2008-2009, the wet period was generally associated with positive anomalies of
183 all indices, whereas the last dry period exhibited negative anomalies in all indices except during rainy days, which
184 showed a weak change.

185 Fig. 3 shows the annual change in % between two consecutive decades of precipitation indices over the Greater
186 Antilles (1985-2015). As shown in fig. 3a, there was an increase in total annual precipitation (PRCPTOT) in
187 southeastern Cuba. This was associated with an increase in the number of rainy days (RR1) (fig.3c) and the average
188 intensity of precipitation per rainy day (SDII) (fig.3c). These results were also observed in Jamaica (fig.3a, 3c). In
189 addition, a decrease in total annual precipitation (PRCPTOT) was observed on the island of Hispaniola (Haiti and the
190 Dominican Republic) (fig.3a). This was associated with a decrease in the average rainfall intensity per wet day (SDII)
191 (fig.3c). This decrease in the SDII was also recorded in Puerto Rico (fig.3c). For heavy precipitation (R95p), as shown
192 in fig.3d, an increase was observed in the southeastern part of Cuba, whereas the whole island (Cuba) was affected by
193 a decrease in wet sequences (CWD) (fig.3e) and dry sequences (CDD) (fig.3f). A decrease in heavy precipitation
194 (R95p) was observed in the central and western regions of Haiti (fig.3d). This was accompanied by an increase in wet
195 sequences (CWD) over Haiti (fig.3e). The Dominican Republic was also affected by this increase in wet sequences
196 (CWD) (fig.3e).



197 Variations in extreme precipitation indices under the influence of variables such as NAO, SOI, TSA, and SST-CAR
198 were analyzed over the Greater Antilles. The influences of large-scale variables were classified as positive, negative,
199 positive, significant, negative, or significant, as shown in figure 4. The results obtained by taking the intersections of
200 the tables presented show the values of the correlation coefficient (with its significance *) between the extreme
201 precipitation indices (PRCPTOT, RR1, SDII, R95p, CWD, and CDD) and the influencing variables (NAO, SOI, TSA,
202 and SST-CAR). The tables in fig. 4 show that NAO has a negative effect on all extremes, while the other SST are
203 positive, except for the number of rainy days (RR1) and the number of consecutive rainy days (CWD). However, the
204 positive phase of the +TSA index had a positive and significant effect on the average rainfall intensity per wet day
205 (SDII), for which a correlation coefficient of 0.37 was obtained. Similarly, with the ONA index, a negative and
206 significant effect ($P < 0.05$) was observed on total annual precipitation (PRCPTOT), average precipitation intensity
207 (SDII), and heavy precipitation (R95p), for which correlation coefficients of 0.49, 0.40, and 0.47, respectively, were
208 obtained.

209 At a local scale, the results show that teleconnections have had positive and significant effects on extreme precipitation
210 indices over the last 30 years in the countries of the Caribbean region, particularly in the Greater Antilles. The spatial
211 extent of significance is indicated by the symbols (*). Thus, a double symbol (**) indicates that the effect extends
212 over a wide area, whereas the effect is limited to that bearing a single symbol (*). The figures ($P \leq 0.05$; fig. 5, 6, 7,
213 8) show the regions or countries over which positive and significant effects were observed for the Greater Antilles.

214 Fig. 5 and suppl. Table 1 shows the effect of the TSA index on extreme precipitation indices (PRCPTOT, RR1, SDII,
215 R95p, CWD, and CDD) in the Greater Antilles. The results show that South Atlantic tropical warming, corresponding
216 to the positive phase of the +TSA index, has a positive and significant effect (**) on the total annual precipitation
217 (PRCPTOT) and heavy precipitation (R95p) in Puerto Rico (fig.5a, 5b; suppl. table1d). In Jamaica, it was also
218 associated with an increase in total annual precipitation (PRCPTOT) and heavy precipitation (R95p) in Puerto Rico
219 (fig.5a, 5b; suppl. table1d). In Haiti, more specifically in the northern part, the increase in the average daily rainfall
220 intensity (SDII) was also associated with +TSA warming (fig.5e; suppl. table1d). In northwest Cuba, this positive
221 phase of +TSA also had a positive and significant effect (**) on mean rainfall intensity per day (SDII) (fig.5e; suppl.
222 table1d). Conversely, in southeastern Cuba, a positive effect was observed for heavy rainfall (R95p) (fig.5b; suppl.
223 table1d).

224 Fig. 6 and suppl. Table 2 shows the effects of warming of the Caribbean Sea surface temperature (SST-Car anomaly,
225 averaged over 14-16N, 65-85 °W) on extreme precipitation in the Greater Antilles. In southern Haiti, an increase in
226 total annual precipitation (PRCPTOT) and the number of rainy days (RR1) was observed as the SST-Car warmed
227 (fig.5a, 5c; suppl. table1a). This increase was also observed for heavy rainfall (R95p) (fig.6b; Suppl. table1a). In
228 eastern Haiti, particularly in Santo Domingo, the positive phase of SST-Car is associated with an increase in the
229 duration of wet sequences (CWD) and the number of rainy days (RR1) (fig.6e, 6c; suppl. table1a). In southeastern
230 Cuba, warming of SST-Car is associated with an increase in total annual precipitation (PRCPTOT) and heavy



231 precipitation (R95p) (fig.6a, 6b; suppl. table1a). An increase in heavy precipitation (R95p) during the positive phase
232 of + SST-Car was also observed in Puerto Rico (fig.6c; Suppl. table1a).

233 Fig. 7 and suppl. table1 show the results of the effect of SOI on extreme precipitation indices (PRCPTOT, RR1, SDII,
234 R95p, CWD, and CDD) in carabid beetles, particularly on the islands forming the Greater Antilles. In Puerto Rico, as
235 shown (fig.7a, 7b; suppl. table1c), the positive phase of the +SOI index was associated with an increase in total annual
236 precipitation (PRCPTOT) and heavy precipitation (R95p). In Haiti, specifically in the south, this positive phase of the
237 +SOI index was associated with an increase in the number of rainy days (RR1), including the duration of wet
238 sequences (CWD) (fig.7c, 7d; suppl. table1c). In Santo Domingo, this is associated with an increase in the duration of
239 wet sequences (CWD) (fig.7d; suppl. table1c). In southeastern Cuba, this is associated with an increase in the average
240 intensity of precipitation per rainy day (SDII) and heavy precipitation (R95p) (fig.7e, 7b; suppl. table1c).

241 Fig. 8 and suppl. table1 show the results of the effect of the NAO index on extreme precipitation indices (PRCPTOT,
242 RR1, SDII, R95p, CWD, and CDD) in the Greater Antilles. The condensed results for different phases of the NAO
243 index are presented in Supplementary Table 1b. In contrast to the results for the other ESS, the positive phase of the
244 +NAO index was only associated with an increase in the number of rainy days (RR1) over Cuba. This increase was
245 greater for coasts facing the Caribbean Sea (fig.8c; Suppl. table1b).

246

247

248 **5. Discussion**

249 The results concerning the effect of the Atlantic Ocean, tropical Pacific, and Caribbean Sea on extreme precipitation
250 indices show that extremes are influenced differently by the oceans and the Caribbean Sea. Moreover, at a local or
251 regional scale, the correlation coefficients measuring trends in this influence are not statistically significant. To clarify
252 these results, we separately discuss the effects of indices (NAO and SOI) and sea surface temperature anomalies (SST-
253 Car, TSA) on extreme precipitation indices.

254 **5.1 Effect of sea surface pressure anomalies (NAO, SOI)**

255 In this study, the effects of the Atlantic Ocean on the Greater Antilles are measured using two indices (NAO and TSA)
256 defined over two ocean areas in two hemispheres. For the Northern Hemisphere, it has been shown that the phases
257 (positive and negative) of the NAO index affect circulation on a Northern Hemisphere scale (Thompson et al., 2000).
258 NAO index results show that the effect produced by the negative phase, corresponding to a weakening of the
259 subtropical anticyclone (Wallace et al., 1981; North Atlantic Oscillation, 2023) and leading to very wet conditions
260 over the Caribbean, particularly the Greater Antilles (Mo et al., 2005; Mestas-Núñez et al., 2007), is associated with
261 a negative effect on all regional extremes. In other words, the NAO index evolves with extremes in the opposite
262 direction, that is, the negative (positive) phase of the NAO is linked to the positive (negative) phase of the precipitation



263 indices. This indicates that the extreme precipitation indices are modulated by the positive and negative phases of the
264 North Atlantic Oscillation (NAO).

265 At a local scale, the effect is observed on all extremes, except for the number of rainy days (RR1). Despite less
266 favorable conditions for precipitation, because the +NAO index is in a positive phase, an increase is recorded on the
267 southern coasts of Cuba and Haiti, whose coastline is the Caribbean Sea.

268 In the case of the SOI, studies have shown that the phenomena induced by phase changes (El Niño, La Niña) have a
269 considerable impact on temperature and precipitation, particularly around the Pacific and Indian oceans (Ropelewski
270 et al., 1987). However, the peri-Atlantic regions are also a concern, as the SOI index is associated with variability in
271 sea surface temperatures and trade wind flows over the tropical Atlantic (Servain (1991); Zebiak (1993)). The positive
272 phase of the +SOI index, manifested by a decrease in the zonal pressure gradient and trade wind flow, leading to
273 persistent cooling in the central equatorial Pacific, result in a non-significant increase in all extremes on a regional
274 scale. However, at a local scale, this positive phase, associated with cold waters in the eastern Pacific (Niña), lead to
275 an increase in the total annual precipitation (PRCPTOT) and heavy precipitation (R95p) in Puerto Rico. It also lead
276 to an increase in the number of rainy days (RR1), including the duration of wet sequences (CWD) in southern Haiti,
277 as well as in the average intensity of precipitation per rainy day (SDII) and heavy precipitation (R95p) in southeastern
278 Cuba. An increase in the duration of wet sequences (CWD) is also observed over the Saint-Dominique region. These
279 results are in line with previous studies showing that a cold Pacific tends to favor precipitation in the Caribbean
280 (Gimeno et al., 2011; Wu et al., 2011; Peterson et al., 2002).

281

282 **5.2 Effect of sea surface temperature anomalies (TSA, SST-Car)**

283 The evolution of temperature anomalies in the South Atlantic (TSA average over 0-20S, 10E-30W) and Caribbean
284 Sea (SST-Car SST average 14-16N, 65-85W) presented in suppl. Fig. 3 are marked by increasing warming in the
285 Atlantic and Caribbean Sea over the period 1985-2015. In the Caribbean, warming has intensified over the past three
286 decades in both seasons (DJF and MAM) (suppl. fig.2). Thus, the +SST-Car phase in the Caribbean is associated with
287 an increase in all extremes at the regional scale, apart from the mean rainfall intensity per wet day (SDII). Similarly,
288 on a local scale, considering all islands, it lead to an increase in the number of consecutive rainy days (CWD), as well
289 as in the number of consecutive rainy days on the island of Hispaniola (Haiti and Santo Domingo). The increase in
290 heavy precipitation (R95p) in Puerto Rico, southeastern Cuba, and Haiti is also due to abnormally warm + SST-Car
291 conditions in the Caribbean. These results are in line with previous research on the influence of sea surface temperature
292 on precipitation in the Caribbean, particularly in the Greater Antilles (Wu et al., 2011), and on the link between sea
293 surface temperature and extreme precipitation indices. For example. It has been shown that the average rainfall
294 intensity per wet day (SDII) averaged over the Caribbean has a strong correlation with the warm phase of the
295 Caribbean Sea (Peterson et al., 2002a). In contrast, the positive +TSA phase (mean TSA over 0-20S, 10E-30W) is
296 associated with warmer sea surface temperatures (SST) in the southern tropical Atlantic (TSA), leading to a southward



297 shift of the ITCZ (Philander et al., 1996) and a weakening of the southeast (SE) trade winds (Schneider et al., 2014;
298 Nobre and Shukla,1996). This warm phase influences the precipitation indices over the Greater Antilles, notably the
299 average daily precipitation intensity (SDII) over the entire region. The same regions, including Puerto Rico, were
300 affected by an increase in heavy precipitation (R95p). In Haiti, the effect is more concentrated on the northwest coast.
301 It is most pronounced in northern Haiti and southeastern Cuba. Similarly, total annual precipitation (PRCPTOT) and
302 heavy precipitation (R95p) in Puerto Rico and Jamaica. These results are compared with those of a previous study
303 (Utida et al., 2019) in which a correlation was found between TSA and precipitation data (rainy season) from CRU
304 TS3.24(Harris et al., 2014). The results show that the warm phase of the TSA influences precipitation in southeastern
305 Cuba and Jamaica. However, the effect is negative over Hispaniola and Puerto Rico. These results confirm that
306 southeastern Cuba and Jamaica were influenced by TSA. The negative effect on Hispaniola could be explained by a
307 less efficient estimation (CRU TS3.24(Harris et al., 2014)) of precipitation due to a grid resolution influenced by
308 topography.

309

310 **5 Conclusion**

311 This work provides a relevant analysis of the evolution of extreme precipitation and its link with global teleconnections
312 over the Caribbean, particularly the Greater Antilles, over the period 1985-2015. Extreme precipitation indices
313 (PRCPTOT, RR1, R95p, CWD, and CDD) defined by the World Meteorological Organization Expert Team on
314 Climate Change Detection and Indices (ETCCDI) were calculated. Next, the links between large-scale SST oscillation
315 indices (NAO, SOI, TSA, and SST-CAR) and extreme precipitation indices (PRCPTOT, RR1, R95p, CWD, and CDD)
316 were evaluated and tested using Spearman's correlation coefficient. The results show that warming in the southern
317 tropical Atlantic (TSA), the Caribbean (mean SST-Car SST 14-16N, 65–85 W), and cooling in the eastern Pacific
318 (Niña) have positive and significant effects on extreme precipitation indices. However, the significant effects on
319 extremes were greatest at the island scale in the Greater Antilles. For example, in southeastern Cuba and Puerto Rico,
320 there was an increase in heavy precipitation (R95p) and average rainfall intensity per wet day (SDII) associated with
321 the positive phase of the indices (SOI, TSA, and SST-Car), whereas in Jamaica and northern Haiti, there were only
322 two indices (TSA and SST-Car). The number of rainy days (RR1) and the maximum duration of consecutive rainy
323 days (CWD) showed a significant upward trend over southern Haiti and the Dominican Republic, in line with the
324 positive phase of the Southern Oscillation (SOI) and warming east of the Caribbean Sea surface.

325 These results further improve our knowledge of the impact of certain global teleconnections on extreme precipitation
326 in the Greater Antilles. They also highlight the most relevant teleconnection indices (SOI, SST-Car (average SST-Car
327 SST 14-16N, 65–85 W), and TSA) to be considered as part of the impact study in the region, to limit damage to key
328 economic sectors such as agriculture, biodiversity, health, and energy.

329



330 **6 Author contribution**

331 Conceptualization: C.D, A.D, S.A; methodology: C.D, A.D, S.A; Original draft preparation: CD; review and editing:
332 all the authors.

333 **7 Competing interests**

334 The authors of this paper declare that they have no conflicts of interest.

335

336

337 **8 Financial supports**

338

339 This research was carried out with the support of the following institutions: 1) ARTS PhD grant from the Institut de
340 Recherche pour le Développement (IRD); 2) Antenor Firmin PhD grant from the French Embassy in Haiti; 3)
341 CARIBACT International Joint Laboratory; 4) CLIMEXHA Project (Anticipation of Extreme CLIMATE events in
342 HAITI for sustainable development).

343

344

345

346 **Bibliography**

Agudelo, P.A., Hoyos, C.D., Curry, J.A., Webster, P.J., 2011. Probabilistic discrimination between large-scale environments of in
decaying African easterly waves. *Clim. Dyn.* 36, 1379–1401. <https://doi.org/10.1007/s00382-010-0851-x>.

Almazroui, Mansour, M. Nazrul Islam, Fahad Saeed, Sajjad Saeed, Muhammad Ismail, Muhammad Azhar Ehsan, Ismaila Diallo, et
Changes in Temperature and Precipitation Over the United States, Central America, and the Caribbean in CMIP6 GCMs.” *Earth
Environment* 5, no. 1 (January 2021): 1–24. <https://doi.org/10.1007/s41748-021-00199-5>.

An, D., Eggeling, J., Zhang, L. et al. Extreme precipitation patterns in the Asia–Pacific region and its correlation with El Ni
Oscillation (ENSO). *Sci Rep* 13, 11068 (2023). <https://doi.org/10.1038/s41598-023-38317-0>.

Baez-Villanueva, O.M.; Zambrano-Bigiarini, M.; Ribbe, L.; Nauditt, A.; Giraldo-Osorio, J.D.; Tinh, N.X. Temporal and spatial
satellite rainfall estimates over different regions in Latin-America. *Atmos. Res.* 2018, 213, 34–50.

Bathelemy R., Brigode P., Boisson D., and Tric E., “Rainfall in the Greater and Lesser Antilles: Performance of five gridded data:
timescale,” *Journal of Hydrology: Regional Studies*, vol. 43, p. 101203, Oct. 2022. <https://doi.org/10.1016/j.ejrh.2022.101203>.

Beharry, Sharlene Lata, Ricardo Marcus Clarke, and Kishan Kumarsingh. “Variations in Extreme Temperature and Precipitation f
Island: Trinidad.” *Theoretical and Applied Climatology* 122, no. 3–4 (November 2015): 783–97. <https://doi.org/10.1007/s00704-0>

Burgess, C.P., Taylor, M.A., Spencer, N. et al. Estimating damages from climate-related natural disasters for the Caribbean at 1.:
global warming above preindustrial levels. *Reg Environ Change* 18, 2297–2312 (2018). <https://doi.org/10.1007/s10113-018-1423-0>.

Chen, Y., Liu, H., An, J., Gorsdorf, U., and Berger, F. H.: A field experiment on the small-scale variability of rainfall based on
micro rain radars and rain gauges, *J. Appl. Meteorol. Clim.*,54, 243–255, 2015.



Cook, K.H., Vizy, E.K., 2010. Hydrodynamics of the Caribbean low-level jet and its relationship to precipitation. *J. Clim.* 23. <https://doi.org/10.1175/2009JCLI3210>.

Curtis, S., and D. W. Gamble. “Regional Variations of the Caribbean Mid-Summer Drought.” *Theoretical and Applied Climatology* (September 2008): 25–34. <https://doi.org/10.1007/s00704-007-0342-0>.

Daly, C., Helmer, E.H., Quiñones, M., 2003. Mapping the climate of Puerto Rico. Vieques Culebra. *Int. J. Clim.* 23. <https://doi.org/10.1002/joc.937>.

Davis, R.E., Hayden, B.P., Gay, D.A., Phillips, W.L., Jones, G.V., 1997. The North Atlantic subtropical anticyclone. *J. Climate* 10, 744. <https://doi.org/10.1175/1520-0442>.

De Giorgi, A., Solarna, D., Moser, G., Tapete, D., Cigna, F., Boni, G., Rudari, R., Serpico, S.B., Pisani, A.R., Montuori, A., et al. Recovery after 2016 Hurricane Matthew in Haiti via Markovian Multitemporal Region-Based Modeling. *Remote Sens.* 20. <https://doi.org/10.3390/rs13173509>.

Dookie, Nalini, Xsitaaz T. Chadee, and Ricardo M. Clarke. “Trends in Extreme Temperature and Precipitation Indices for the Caribbean Islands: Trinidad and Tobago.” *Theoretical and Applied Climatology* 136, no. 1–2 (April 2019): 31–44. <https://doi.org/10.1007/s00704-018-2463-z>.

Enfield DB, Mestas-Nunez AM, Trimble PJ. 2001. The Atlantic multidecadal oscillation and its relation to rainfall and river discharge over the continental US. *Geophys. Res. Lett.* 28: 2077–2080. <http://dx.doi.org/10.1029/2000GL012745>.

Funk, C.; Peterson, P.; Landsfeld, M.; Pedreros, D.; Verdin, J.; Shukla, S.; Husak, G.; Rowland, J.; Harrison, L.; Hoell, A.; et al. A new environmental record for monitoring extremes. *Sci. Data* 2015. <https://doi.org/10.1038/sdata.2015.66>.

Funk, C., Verdin, A., Michaelsen, J., Peterson, P., Pedreros, D., and Husak, G.: A global satellite-assisted precipitation climatology. *Sci. Data* (2015a), 7, 275–287. <https://doi.org/10.5194/essd-7-275-2015>.

Frich, P., L. V. Alexander, P. Della-Marta, B. Gleason, M. Haylock, A. Klein Tank, and T. Peterson, Observed Coherent Changes in Extremes during the Second Half of the Twentieth Century, *Clim. Res.*, 19, 193 – 212, 2002. <http://dx.doi.org/10.3354/cr019193>.

Gimeno L, Magaña V, Enfield DB. 2011. Introduction to special section on the role of the Atlantic warm pool in the climate of the Caribbean Hemisphere. *J. Geophys. Res.* 116:D00Q01. <https://doi.org/10.1029/2011JD016699>.

Griffiths, J.F. and Driscoll, J.M. 1982: Survey of climatology. Columbus, OH: Charles Merrill.

Hall, Trevor C., Andrea M. Sealy, Tannecia S. Stephenson, Shoji Kusunoki, Michael A. Taylor, A. Anthony Chen, and Akio Kamekura. “Climate of the Caribbean from a Super-HighResolution Atmospheric General Circulation Model.” *Theoretical and Applied Climatology* 1–2 (July 2013): 271–87. <https://doi.org/10.1007/s00704-012-0779-7>.

Harris, I., Jones, P. D., Osborn, T. J. & Lister, D. H. Mise à jour des grilles à haute résolution des observations climatiques mensuelles et données CRU TS3.10. *J. Climatol.* 34, 623-642. <https://doi-org.insu.bib.cnrs.fr/10.1002/joc.3711> (2014).



Hastenrath, S., 2002. The intertropical convergence zone of the eastern Pacific revisited. *Int. J. Climatol.* 2
<https://doi.org/10.1002/joc.739>.

Huang, B., C. Liu, V. Banzon, E. Freeman, G. Graham, B. Hankins, T. Smith, and H.-M. Zhang, 2021: Improvements of the D Interpolation Sea Surface Temperature (DOISST) Version 2.1, *Journal of Climate*, 34, 2923-2939.

Hurrell JW. Decadal trends in the north atlantic oscillation: regional temperatures and precipitation. *Science*. 1995 Aug 4;269
<https://doi.org/10.1126/science.269.5224.676>.

Inter-American Development Bank. (2014). *Climate change and IDB: building resilience and reducing emissions; regional study island developing states*.

IPCC. 2007. *Climate Change 2007: Synthesis Report*. Working Group, I, II and III contributions to the Fourth Assessment Report. <http://www.ipcc.ch>.

Jones, P.D., Jónsson, T. and Wheeler, D., 1997: Extension to the North Atlantic Oscillation using early instrumental pressure observations from Gibraltar and South-West Iceland. *Int. J. Climatol.* 17, 1433-1450.

Joseph, P : *La Caraïbe, données environnementales*. Coordonné par Joseph P. Karthala, Paris, et Géode (Groupe de recherche développement, environnement de la Caraïbe), Éditions KARTHALA. 458p, 2006.

Khadgarai, S.; Kumar, V.; Pradhan, P.K. The Connection between Extreme Precipitation Variability over Monsoon Asia and Circulation Patterns. *Atmosphere* 2021, 12, 1492. <https://doi.org/10.3390/atmos12111492>.

Mariani, M., Holz, A., Veblen, T. T., Williamson, G., Fletcher, M.-S., & Bowman, D. M. J. S. (2018). Climate change amplification of fire teleconnections in the Southern Hemisphere. *Geophysical Research Letters*, 45. <https://doi.org/10.1029/2018GL078294>.

Martens, B., Waegeman, W., Dorigo, W.A. et al. Terrestrial evaporation response to modes of climate variability. *npj Clim Atmos Earth Syst Sci* (2018). <https://doi.org/10.1038/s41612-018-0053-5>.

Mestas-Núñez, A. M., D. B. Enfield, and C. Zhang, 2007: Water vapor fluxes over the Intra-Americas Sea: Seasonal and interannual variability and associations with rainfall. *J. Climate*, 20, 1910–1922.

McLean, Natalie Melissa, Tannecia Sydia Stephenson, Michael Alexander Taylor, and Jayaka Danaco Campbell. “Characterizing Caribbean Rainfall and Temperature Extremes across Rainfall Zones.” *Advances in Meteorology* 2015 (2) <https://doi.org/10.1155/2015/425987>.

Mo, K. C., M. Chelliah, M. L. Carrera, R. W. Higgins, and W. Ebisuzaki, 2005: Atmospheric moisture transport as evaluated from the National Centers for Environmental Prediction Reanalysis and forecast products. *J. Hydrometeorol.*, 6, 710–728.

Moron, V., Frelat, R., Jean-Jeune, P.K., Gaucherel, C., 2015. Interannual and intra-annual variability of rainfall in Haiti (1905–2005). *Journal of Climate*, 28, 915–932. <https://doi.org/10.1007/s00382-014-2326-y>.

Naciones Unidas, Comisión Económica para América Latina y el Caribe, 1988, República Dominicana : evaluación de los daños por el huracán Georges, 1998, sus implicaciones para el desarrollo del país, 91p.

Nobre, P. and Shukla, J. (1996) Variation of Sea Surface Temperature, Wind Stress and Rainfall over the Tropical Atlantic and Southern Ocean. *Journal of Climate*, 9, 2464-2479. <http://dx.doi.org/10.1175/1520-0442>.



North Atlantic Oscillation, NOAA's Climate Prediction Center. Accessed December 8, 2023.

Love, T. B., Kumar, V., Xie, P. & Thiaw, W. A 20-year daily Africa precipitation climatology using satellite and gauge data. In P the 84th AMS Annual Meeting, Conference on Applied Climatology, Seattle, (2004).

Panamerican Health Organisation 2019 Assessment of the effects and impacts of hurricane dorian in the bahamas Technical report DC : PHO).

Peterson, T. C., C. Folland, G. Gruza, W. Hogg, A. Mokssit, and N. Plummer, Report of the activities of the Working Group on CI Detection and related rapporteurs, World Meteorol. Organ. Tech. Doc. 1071, 143 pp., Comm. for Climatol., World Meteorol. Or 2001.

Peterson, Thomas C., Michael A. Taylor, Rodger Demeritte, Donna L. Duncombe, Selvin Burton, Francisca Thompson, Avalor "Recent Changes in Climate Extremes in the Caribbean Region: RECENT CHANGES IN CLIMATE EXTREMES IN THE C REGION." Journal of Geophysical Research: Atmospheres 107, no.D21(November 16, 2002a): ACL 16-1 <https://doi.org/10.1029/2002JD002251>.

Philander, S., Gu, D., Lambert, G. & Li, T. Why the ITCZ is mostly north of the equator. J. Climate 9, 2958–2972(1996) org.insu.bib.cnrs.fr/10.1175/1520-0442.

Rodrigues, M., Peña-Angulo, D., Russo, A., Zúñiga-Antón, M. & Cardil, A. Do climate teleconnections modulate wildfire-prone c the Iberian Peninsula? Environ. Res. Lett. 16, 044050 (2021).

Ropelewski C. F. et M. S. Halpert, 1987: Global and regional scale precipitation and temperature patterns associated with El Niñ Oscillation. Mon. Wea. Rev., 115, 1606-1626.

Servain J., 1991: Simple climatic indices for the Tropical Atlantic Ocean. *J. Geophys. Res.*, 96, C8, 15, 137-146.

Schneider, T., Bischoff, T. & Haug, G. Migrations and dynamics of the intertropical convergence zone. Nature 513(7516), 45–5 org.insu.bib.cnrs.fr/10.1038/nature13636 (2014).

Stephenson, Tannecia S., Lucie A. Vincent, Theodore Allen, Cedric J. Van Meerbeeck, Natalie McLean, Thomas C. Peterson, Mich et al. "Changes in Extreme Temperature and Precipitation in the Caribbean Region, 1961–2010." International Journal of Climato (July 2014): 2957–71. <https://doi.org/10.1002/joc.3889>.

Sunilkumar, K.; Narayana Rao, T.; Satheshkumar, S. Assessment of small-scale variability of rainfall and multi-satellite precipita using measurements from a dense rain gauge network in Southeast India. Hydrol. Earth Syst. Sci. 2016, 20, 1719–1735.

Taylor, Michael A., Leonardo A. Clarke, Abel Centella, Arnoldo Bezanilla, Tannecia S. Stephenson, Jhordanne J. Jones, Jayaka Alejandro Vichot, and John Charlery. "Future Caribbean Climates in a World of Rising Temperatures: The 1.5 vs 2.0 Dilemm Climate 31, no. 7 (April 2018): 2907–26. <https://doi.org/10.1175/JCLI-D-17-0074.1>.

Taylor MA, Enfield DB, Chen AA. 2002a. The influence of the tropical Atlantic vs. the tropical Pacific on Caribbean rainfall. J. C (107(C9): 3127. <https://doi:10.1029/2001JC001097>.

Thompson, D. W. J., and J. M. Wallace, Annular modes in the extratropical circulation Part I: Month- to-month variability, J. Cl 1000–1016, 2000. [https://doi.org/10.1175/1520-0442\(2000\)013<1000:AMITEC>2.0.CO;2](https://doi.org/10.1175/1520-0442(2000)013<1000:AMITEC>2.0.CO;2).



Thorncroft, C., Hodges, K., 2001. African easterly wave variability and its relationship to atlantic tropical cyclone activity. *J. Cl* 1179. [https://doi.org/10.1175/1520-0442\(2001\)014](https://doi.org/10.1175/1520-0442(2001)014).

Utida, G., Cruz, F., Etourneau, J. et al. Tropical South Atlantic influence on Northeastern Brazil precipitation and ITCZ displacem past 2300 years. *Sci Rep* 9, 1698 (2019). <https://doi-org.insu.bib.cnrs.fr/10.1038/s41598-018-38003-6>.

Vichot-Llano, Alejandro, Daniel Martinez-Castro, Arnoldo Bezanilla-Morlot, Abel CentellaArtola, and Filippo Giorgi. "Project Precipitation and Temperature Regimes and Extremes over the Caribbean and Central America Using a Multiparameter Ensemble International Journal of Climatology 41, no. 2 (February 2021): 1328–50. <https://doi.org/10.1002/joc.6811>.

Wallace, J. M., and D. S. Gutzler, 1981: Teleconnections in the geopotential height field during the Northern Hemisphere Winte *Rev.*, 109, 784-812.

Wu, R., Kirtman, B.P. Caribbean Sea rainfall variability during the rainy season and relationship to the equatorial Pacific and trc SST. *Clim Dyn* 37, 1533–1550 (2011). <https://doi.org/10.1007/s00382-010-0927-7>.

Zebiak S., 1993: Air-Sea interactions in the equatorial Atlantic region. *J. Climate*, 6, 1567-1586.

1.

347
348
349

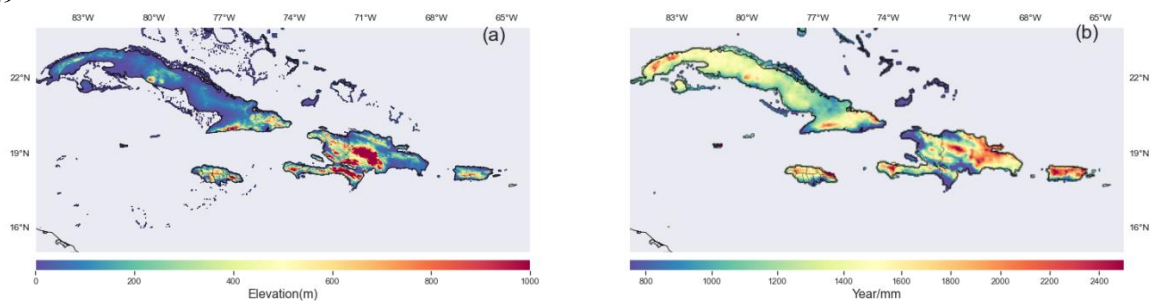
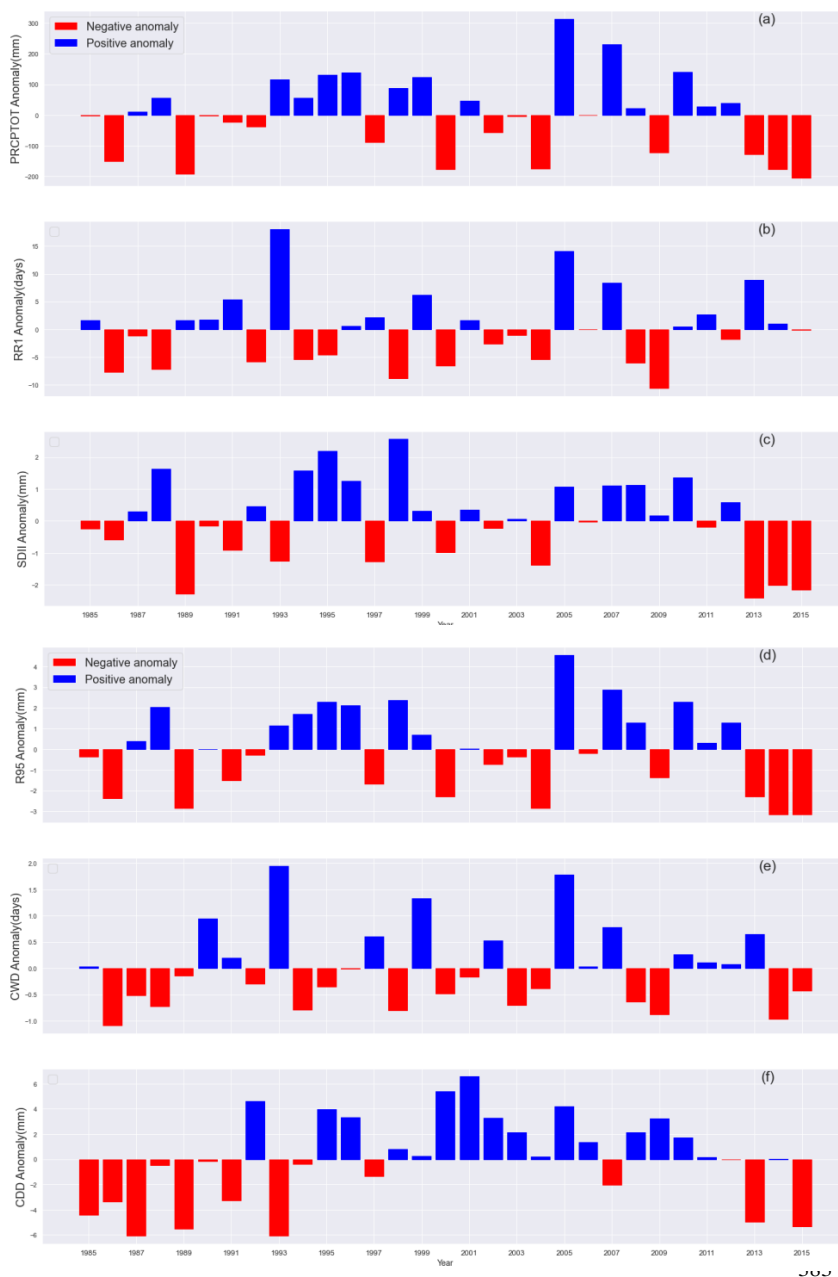
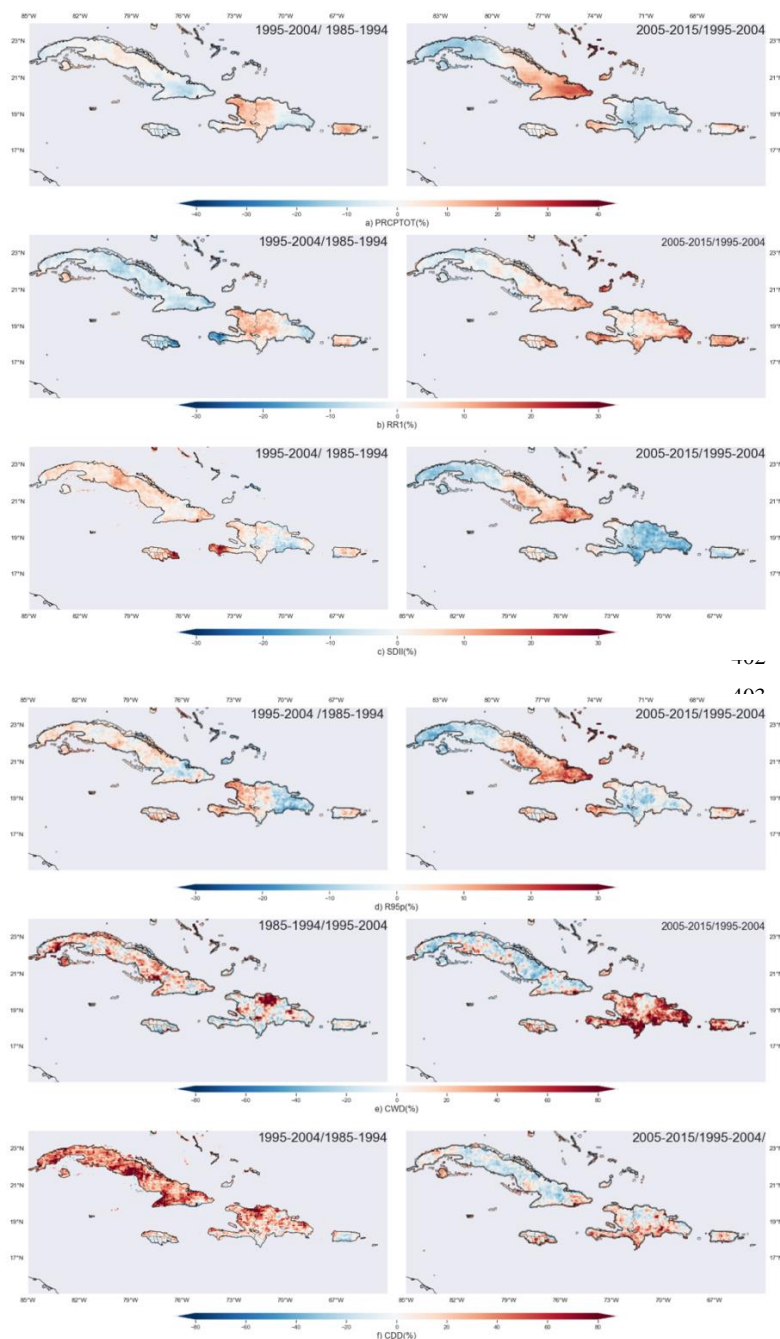


Figure 1. Location of study area. The figures show (a) the altitude of the four islands making up the Greater Antilles and (b) average annual rainfall.

350



384 Figure 2. Interannual variability of precipitation indices in the Greater Antilles over period 1980-2015 with (a) PRCPTOT, (b)
385 RR1, (c) SDII, (d) R95; (e) CWD; (f) CDD.

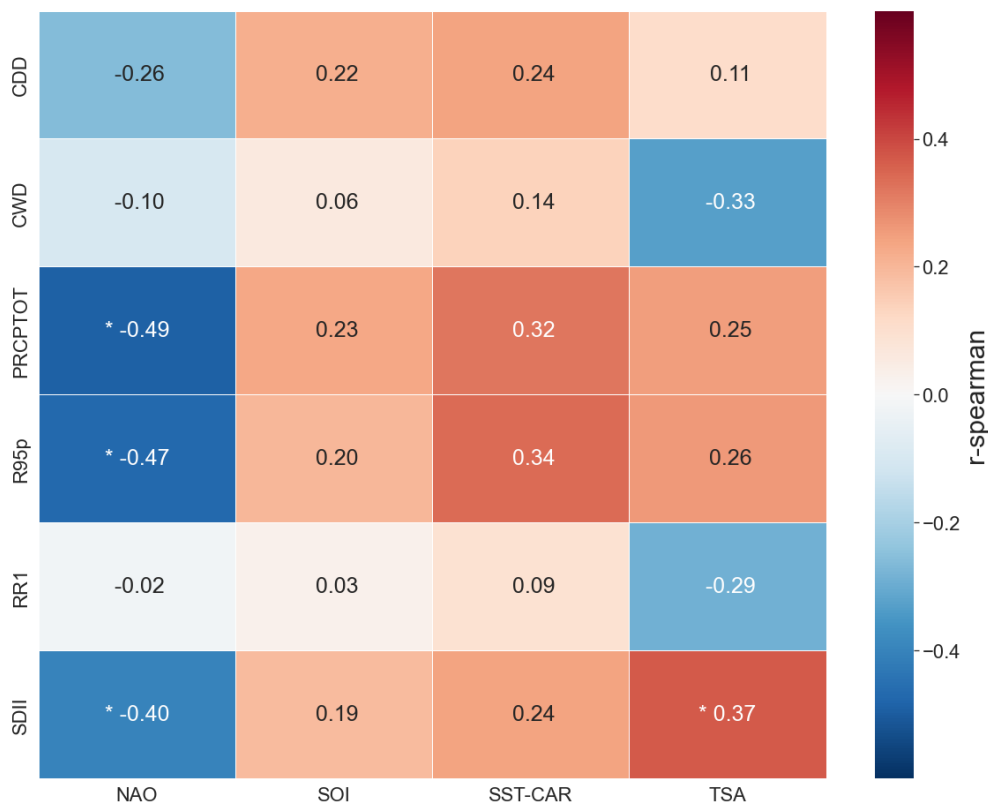


420

421 Figure 3. Annual change (%) between two decades of precipitation indices over the Greater Antilles (left: 1995-2004 compared
422 to 1985-2015; right: 2005-2015 compared to 1995-2004 right): (a) PRCPTOT, (b) RR1, (c) SDII, (d) R95p, (e) CWD (f) CDD.
423



424
 425
 426
 427



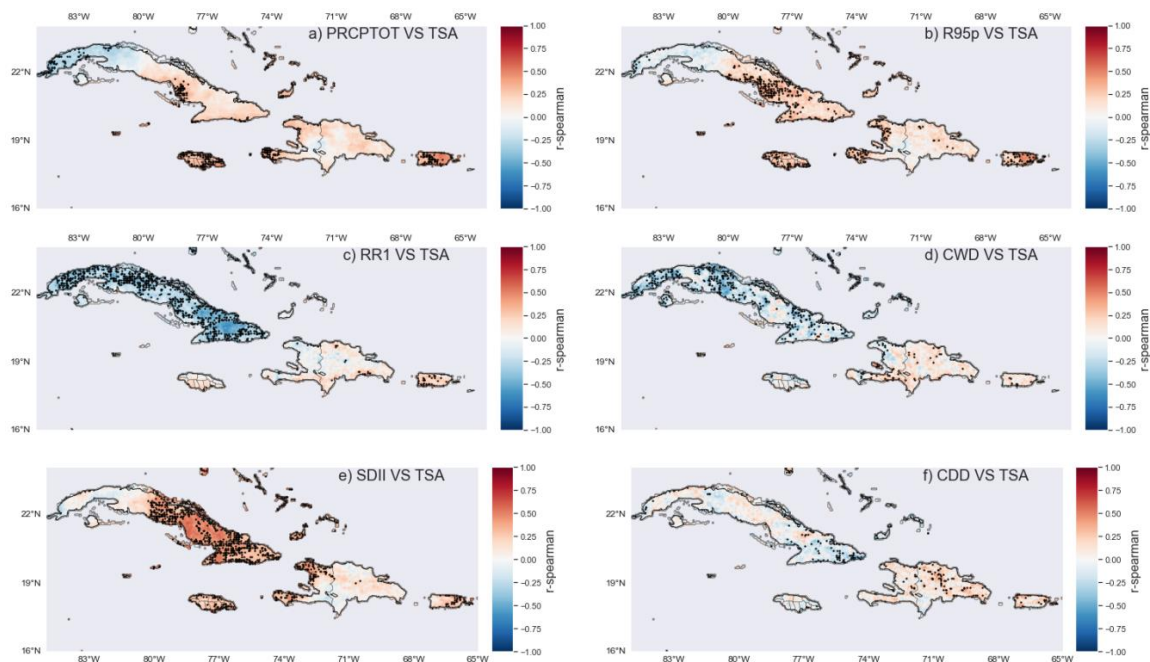
428
 429
 430
 431
 432
 433
 434
 435
 436
 437
 438
 439
 440

Figure 4. Correlation between precipitation indices and large-scale SST in the Greater Antilles (1985-2015). The values in table are the correlation coefficients of large-scale SST with extremes. The indices on the abscissa are the precipitation extremes and those on the ordinate are the SST indices. The symbol (*) represents a statistically significant correlation at a threshold less than or equal to 0.05.



441

442



443

Figure 5. Correlation between precipitation indices and Tropical Southern Atlantic Index (TSA). The spatial correlation of extremes with TSA (SST average over 0-20S, 10E-30W) for this figure is presented in two columns; the first is realized with the indices: a) PRCPTOT Corr. TSA, b) RR1 Corr. TSA, c) SDII Corr. TSA and the second column with the indices: b) R95p Corr. TSA, d) CWD Corr. TSA, f) CDD Corr. TSA. Black dots represent areas where correlations are statistically significant at $p < 0.05$.

444

445

446

447

448

449

450

451

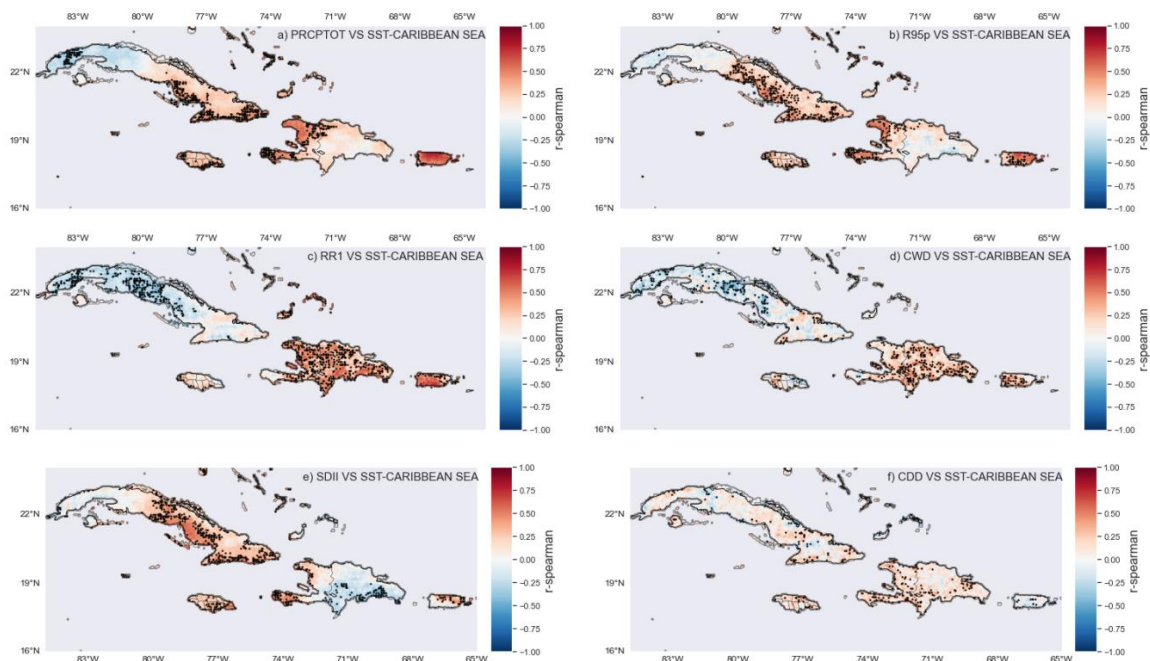
452

453

454



455



456

Figure 6. Correlation between precipitation indices and Caribbean Sea surface temperature. The spatial correlation of extremes with SST-Car(SST average 14-16N, 65-85W) for this figure is presented in two columns; the first is realized with the indices: a) PRCPTOT Corr. SST-Car, b) RR1 Corr. SST-Car, c) SDII Corr. SST-Car and the second column with the indices: b) R95p Corr. SST-Car, d) CWD Corr. SST-Car, f) CDD Corr. SST-Car. Black dots represent areas where correlations are statistically significant at $p < 0.05$.

457

458

459

460

461

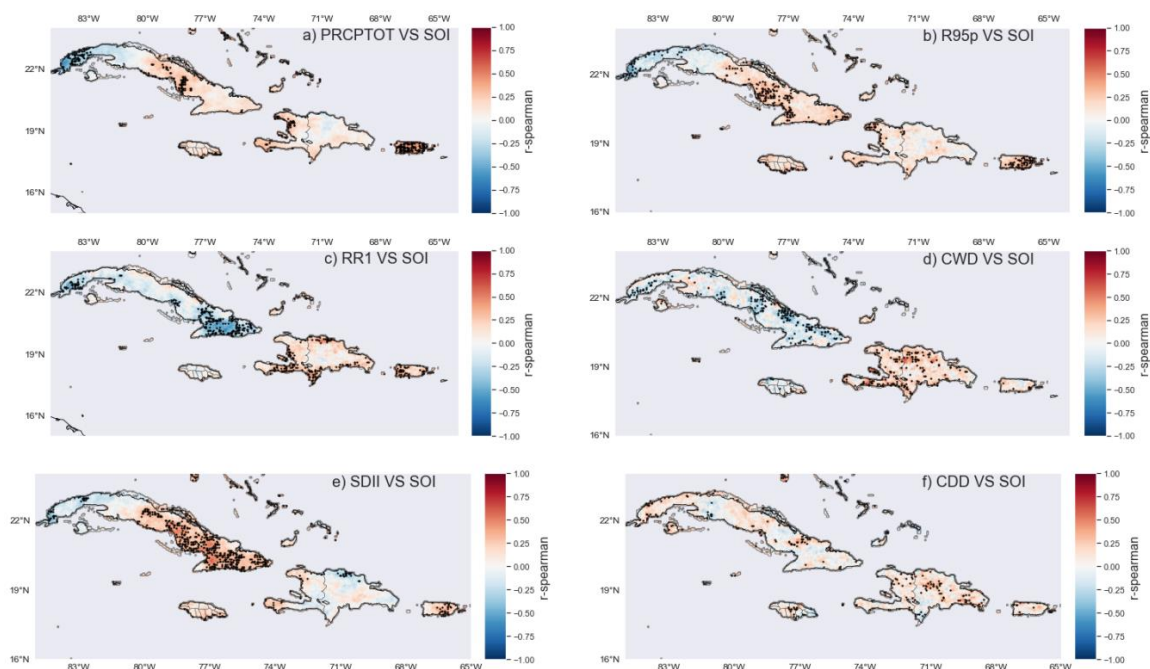
462

463

464



465



466

Figure 7. Correlation between precipitation indices and Southern Oscillation indices (SOI). The spatial correlation of extremes with SOI for this figure is presented in two columns; the first is realized with the indices: a) PRCPTOT Corr. SOI, b) RR1 Corr. SOI, c) SDII Corr. SOI and the second column with the indices: b) R95p Corr. SOI, d) CWD Corr. SOI, f) CDD Corr. SOI. Black dots represent areas where correlations are statistically significant at $p < 0.05$.

467

468

469

470

471

472

473

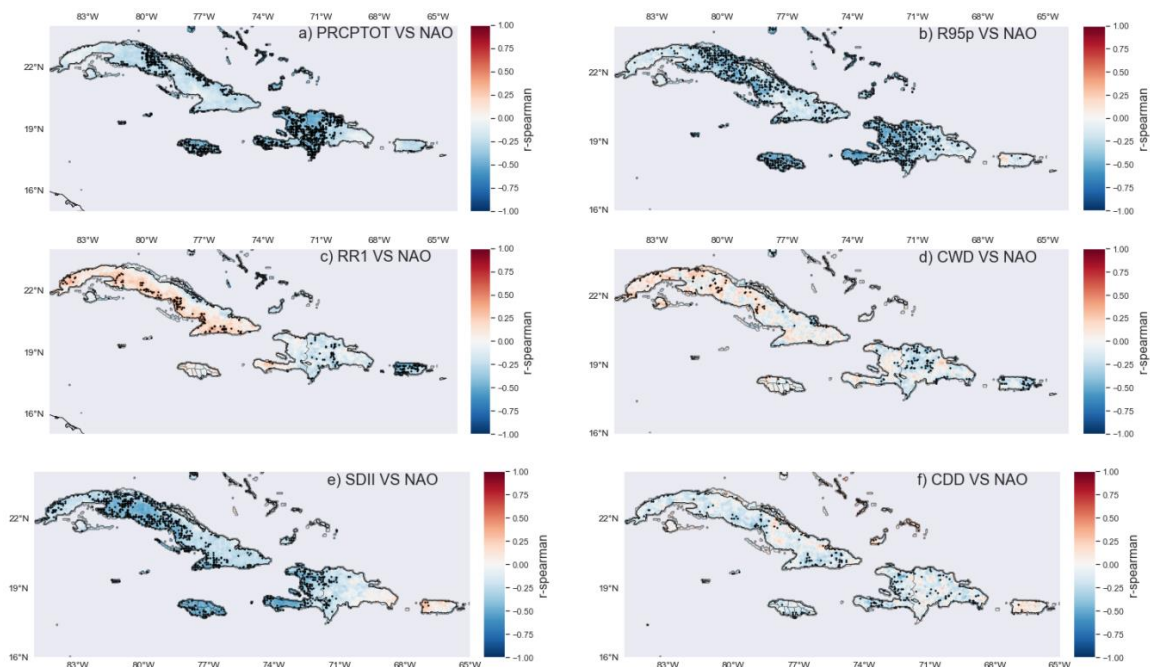
474

475

476



477



478

Figure 8. Correlation between precipitation indices and North Atlantic Oscillation Indices (NAO). The spatial correlation of extremes with NAO for this figure is presented in two columns; the first is realized with the indices: a) PRCPTOT Corr. NAO, b) RR1 Corr. NAO, c) SDII Corr. NAO and the second column with the indices: b) R95p Corr. NAO, d) CWD Corr. NAO, f) CDD Corr. NAO. Black dots represent areas where correlations are statistically significant at $p < 0.05$.

479



480

481

482

483 **Table 1** Precipitation indices

ID	Index Name	Indices definition	Units
RR1	Wet days index	Number of wet days $\geq 1\text{mm}$	days
PRCPTOT	Annual total wet day precipitation	Annual total rainfall $\geq 1\text{mm}$	mm
SDII	Simple daily rainfall intensity index	Annual total precipitation divided by the number of wet days (defined as precipitation $\geq 1.0\text{ mm}$) in the year	mm/days
CWD	Consecutive wet days	Maximum number of consecutive days with daily rainfall $\geq 1\text{mm}$	days
CDD	Consecutive dry days	Maximum number of consecutive days with daily rainfall $< 1\text{mm}$	days
R95p	Very wet days.	Annual total PRCP when RR>95th percentile.	mm

484

485

486